A major purpos
cal Information Cen
the broadest diss
ble of informatio
DOE's Research a
Reports to busines
academic communi
state and local gov

Although a sma
report is not rep
being made availa
the availability of in
research discussed

of the report
is to provide
ination possi-
contained in
Development
industry, the
and federal,
ments.
portion of this
ducible, it is
to expedite
mation on the
erein.

CONF-840616--19

Los Alamos National Laboratory is operated by the University of California for the United States Department of Energy under contract W-7405-ENG-36.

TITLE: THE PHYSICS OF REVERSED-FIELD PINCH PROFILE SUSTAINMENT

LA-UR--84-2023

DE84 014024

AUTHOR(S): R. W. Moses

SUBMITTED TO: International Conference on Plasma Physics
Lausanne, Switzerland (June 27-July 3, 1984)

DISCLAIMER

Los Alamos National Laboratory
Los Alamos, New Mexico 87545

FORM NO 836 R4
ST NO 2629 5/81

THE PHYSICS OF REVERSED-FIELD PINCH PROFILE SUSTAINMENT

R. W. Moses

Los Alamos National Laboratory
Los Alamos, New Mexico 87545 USA

ABSTRACT

A description of the Reversed-Field Pinch (RFP) is given, emphasizing the necessity of a magnetohydrodynamic (MHD) or kinetic process to sustain field reversal. Three sustainment mechanisms are reviewed: the MHD dynamo, the tangled discharge model, and nonlocal resistivity. A slab model of steady (ohmic) states is described. A relationship between ohmic state wave numbers and the minimum amplitude of nonsymmetric field components is given. If ohmic states are the sole source of the sustainment process, their wave lengths are probably much longer than the minor diameter of the plasma. Otherwise field asymmetries would exceed those observed in experiments. It is noted that internal field data are still limited, restricting the generality of our comments.

*Work performed under the auspices of the USDOE.

1. Introduction

The Reversed-Field Pinch (RFP) /1,2/ is a toroidally symmetric device, uniquely characterized by the reversal of the toroidal magnetic field on the plasma surface as compared to the magnetic field on the minor axis. The enhanced plasma stability and quiescent RFP operation during field reversal have drawn the attention of plasma physics researchers for many years /3/. Also noted on early RFPs was the phenomenon of "self-reversal" /4/. The poloidal plasma currents necessary for field reversal are developed without the poloidal electric fields required by one-dimensional diffusion models. This phenomenon is often referred to as the "dynamo effect." A conceptualization of RFP current, field, and power flow is shown in Fig. 1.

A physical explanation of RFP behavior was presented by Taylor /5/. He suggested that magnetic field energy in a plasma, $W = (1/2\mu_0) \int B^2 dV$, will decay more rapidly than magnetic helicity, $K = \int \underset{\sim}{A} \cdot \underset{\sim}{B} dV$. This leads to the force-free plasma model that satisfies

$$\nabla \times \underset{\sim}{B} = \mu \underset{\sim}{B} \quad , \tag{1}$$

where μ is a constant. When the RFP is treated as a straight cylinder, Eq. (1) is solved by $B_z(r) = B_0 J_0(\mu r)$ and $B_\theta = B_0 J_1(\mu r)$. The Bessel function model (BFM) is compared with experiment best by matching the respective $F - \Theta$ curves where $F = B_z(a)/\bar{B}$, $\Theta = B_\theta(a)/\bar{B}$, $\bar{B}$ = volume averaged B_z, and a = plasma radius. A comparison of experiment and theory is shown in Fig. 2 where the BFM is compared to the results of a 180 kA shot on ZT-40M /6/. In this typical example, Θ values for ZT-40M are about 20% higher than those of the BFM for the same values of F. This good greement between experiment and theory has been observed in many RFPs and is taken as strong support for the Taylor theory.

Many people have introduced new concepts to "fine tune" the Taylor model or add to our detailed understanding of the RFP. For example the modified Bessel function model (MBFM) /7,8/ replaces the constant μ in Eq. (1) with a variable $\mu(r)$, see Fig. 3. This is motivated by the idea that low plasma temperatures near the wall would increase resistivity, η, and reduce currents there. Thus, $\mu(r)$ is constant in the plasma interior but small in the edge region. There is some direct field measurement evidence for this in OHTE /9/. The extra freedom of the MBFM allows us to match the experimental $F - \Theta$ curve precisely, /10/ see Fig. 4. It has been observed that the

departure of the F - Θ curve from the Taylor model has significant ramifications for RFP physics. The 20% difference in Θ between the BFM of Fig. 2 and the MBFM of Fig.4 indicates that ~70% of the input power is dissipated ohmically by "mean" currents while ~30% of the input power goes to fluctuations /10/. In the same analysis it was also concluded that the parallel resistivity, $\eta_{\parallel}$, agrees with the Spitzer formula /11/ within the limits of experimental error.

While the forementioned theories explain some aspects of RFP formation and transport, other theories delve into the intricate nature of RFP plasma and field profiles. Statistical theories /12,13/ based on the Gibbs hypothesis give added physical meaning to the BFM and explain the observation that many RFPs tend to operate best at Θ = 1.56. It is even possible to estimate magnetic field fluctuation autocorrelation lengths with a statistical model /13/.

Despite the many successes of RFP theory, two aspects remain incomplete and highly controversial: the "dynamo effect" and thermal/particle transport. In the rest of this paper we explore three possible mechanisms of RFP profile sustainment (dynamo) and comment on their relation to transport.

2. Profile Sustainment Models

As mentioned earlier, the phenomenon of self-reversal during RFP startup was seen as evidence of an RFP dynamo. In early RFPs the toroidal current, $I_z = 2\pi\int_0^a J_z(r)rdr$, and flux, $\Phi(r) = 2\pi\int_0^r B_z(r)rdr$, were allowed to decay slowly after the startup phase of the experiment. Once Φ begins to decay, toroidal flux can drive a poloidal current by diffusion

$$\eta J_\theta(r) = -\frac{1}{2\pi r}\frac{\partial\Phi(r)}{\partial t} = E_\theta(r) \quad , \tag{2}$$

where η is the plasma resistivity.

With the development of driven RFPs, I_z can be held constant as long as the transformer can produce a toroidal loop voltage, V_z. In the case of ZT-40M, I_z and Φ may be effectively constant for over 10 ms while $V_z \approx 40$ V /14/. When I_z and Φ are held constant, the right-hand side of Eq. 2 is effectively zero. Detailed studies of ZT-40M and diffusion theory /14,15/ have indicated that no one-dimensional manipulation of plasma

profiles can alleviate this paradox. As in the case of self-reversal, one must find additional terms to drive J_θ in Eq. (2), in place of E_θ.

2.1. The MHD Dynamo

The most extensive studies of RFP profile sustainment are based on the MHD dynamo described by Moffatt /16/. Ohm's law in the presence of plasma velocity $\underset{\sim}{u}$ may be written as follows:

$$\underset{\sim}{E} + \underset{\sim}{u} \times \underset{\sim}{B} = \eta \underset{\sim}{J} \quad . \tag{3}$$

In the notation of Ref. 10 we separate variables into time or spatial averages, $\langle\ \rangle$, and fluctuating parts, δ. Typical examples are $\underset{\sim}{B} = \langle \underset{\sim}{B} \rangle + \delta \underset{\sim}{B}$ and $\underset{\sim}{E} = \langle \underset{\sim}{E} \rangle + \delta \underset{\sim}{E}$. Furthermore a mean of a linear fluctuation is always zero, for example $\langle \delta \underset{\sim}{E} \rangle = 0$; but the mean of a product of fluctuations is usually nonzero, $\langle \delta \underset{\sim}{u} \times \delta \underset{\sim}{B} \rangle \neq 0$. This leads to the obvious additional term to resolve the paradox of Eq. (2)

$$\eta \langle J_\theta \rangle = - \frac{1}{2\pi r} \frac{\partial \Phi(r)}{\partial t} + \langle \delta \underset{\sim}{u} \times \delta \underset{\sim}{B} \rangle_\theta \quad . \tag{4}$$

The MHD dynamo is an excellent candidate for driving field reversal in the RFP if $\langle \delta \underset{\sim}{u} \times \delta \underset{\sim}{B} \rangle$ can be large enough to sustain $\eta \langle J_\theta \rangle$ in the absence of $\partial \Phi(r)/\partial t$.

Several authors have demonstrated theoretically that the MHD dynamo can form and/or sustain an RFP field profile. The first to observe this numerically were Sykes and Wesson /17/ using a 3D MHD code on a $14 \times 14 \times 13$ mesh. They obtained field reversal in the presence of very large field fluctuations. Schnack /18/ and Aydemir and Barnes /19/ also have observed dynamo action with 3D MHD codes. Of particular interest in their work is the helical ohmic state. In this case the magnetic field is constant in time. The dynamo is driven by steady plasma velocities and spatial fluctuations of $\underset{\sim}{B}$.

Caramana, Nebel, and Schnack /20/ have used a 3D code to model the sawtooth crash seen in high Θ operation of ZT-40M /21/. Werley and Nebel /22/ have shown that no dynamo action is needed during the sawtooth rise. The code results /19/ also indicate that the dynamo has a very

different character at low Θ. In that instance sawtoothing is not observed and good flux surfaces may exit at the reversal layer near the plasma edge.

More recently Strauss /23/ has formulated a set of reduced equations to describe the RFP. He has observed the dynamo effect in a plasma with field fluctuations $|\delta\underline{B}|/\langle B\rangle < 10\%$.

Ordinarily one might conclude that these observations would "close the book" on RFP sustainment, indicating that it is strictly caused by the MHD dynamo. However, there are concerns that the MHD model does not account for all sustainment processes. First, the field fluctuations seem to be too high. Unless a model is run with very little reversal, or close to a paramagnetic state, /19/ the field fluctuations are typically $|\delta\underline{B}|/\langle B\rangle \sim 7\text{-}10\%$. RFP experiments usually operate with $|\delta\underline{B}|/\langle B\rangle$ at the plasma edge $\lesssim 5\%$ /10/. Second, the F - Θ curves of the codes are often too far to the right of the experiment. Third, the models are often far more stochastic than the machines /24/. If magnetic field line stochasticity reaches from the plasma interior to the wall in a model with long wavelength modes, each field line may travel only ~10-40 m before it hits the wall. Meanwhile, to account for estimated particle loss rates due to parallel transport in ZT-40M, one needs field lines that are several hundred meters long. /25/ We will attempt to quantify these concerns and relate the MHD dynamo to other sustainment models in Sec. III and Sec. IV, respectively.

2.2 The Tangled Discharge Model

The Tangled Discharge Model (TDM) developed by Rusbridge /26/ is based on the assumption that magnetic field lines, or flux tubes, wander stochastically throughout the plasma. It is also assumed that plasma current is constrained to flow along the same channels as the magnetic field so that Eq. (1) is satisfied everywhere in the machine. Consequently, the mean field $\langle\underline{B}\rangle$ satisfies the BFM, but the fluctuations generate stochasticity and prevent the development of any good flux surfaces.

The stochastic wandering of current makes it possible for a current channel to pick up the induced toroidal loop voltage V_z as it moves near the minor axis of the RFP. Then the current channel can wander to the reversal region where induced toroidal voltage is redirected to drive a poloidal current, as if it were a solid, insulated conductor.

The TDM can be represented mathematically when a distinction is made between plasma resistivity parallel to the magnetic field, $\eta_\parallel$, and

resistivity perpendicular to the field, $\eta_\perp$. Ohm's law is modified to read as follows:

$$\underset{\sim}{E} + \underset{\sim}{u} \times \underset{\sim}{B} = \eta_\perp \underset{\sim}{J} - (\eta_\perp - \eta_\parallel) \frac{\underset{\sim}{J} \cdot \underset{\sim}{B}}{B^2} \underset{\sim}{B} \quad . \tag{5}$$

If $\eta_\perp$ is taken to be much larger than $\eta_\parallel$, it is possible to choose fluctuating components of $\underset{\sim}{B}$ and $\underset{\sim}{J}$ and sustain poloidal current as follows

$$\eta_\parallel \langle J_\theta \rangle \simeq - \frac{1}{2\pi r} \frac{\partial \Phi(r)}{\partial t} + \langle \delta \underset{\sim}{u} \times \delta \underset{\sim}{B} \rangle$$

$$+ (\eta_\perp - \eta_\parallel) \left[\frac{\langle \delta \underset{\sim}{J} \cdot \delta \underset{\sim}{B} \rangle}{B^2} \langle \underset{\sim}{B} \rangle \right.$$

$$\left. + \langle \delta(\underset{\sim}{J} \cdot \underset{\sim}{B}) \cdot \delta(\underset{\sim}{B}/B^2) \rangle \right] \quad . \tag{6}$$

In this model one could eliminate both toroidal flux decay and plasma flow and still maintain field reversal.

We hesitate to use the TDM as a primary model of RFP sustainment bec use it relies so heavily on the unproven condition $\eta_\perp / \eta_\parallel >> 1$. We do find that combining the concept of stochastic magnetic fields with a Boltzman treatment of electron momentum leads to a more general model of RFP sustainment, as discussed in the next section.

2.3. Nonlocal Resistivity

The model of nonlocal plasma resistivity proposed by Jacobson and Moses /27/ incorporates the concept of magnetic field line stochasticity discussed by many other authors, /28,29/ including Rusbridge /26/. To avoid the complexity of having trapped particles, this model was presented in slab geometry with $\beta = 0$, so that $B = |\underset{\sim}{B}|$ is approximately uniform in space. The magnetic axis of the cylindrical model becomes the $x = 0$ plane of the slab model. The plasma boundary is now at $x = \pm a$. As in the case of the cylinder, the driving electric field is $\langle \underset{\sim}{E} \rangle = E_0 \hat{z}$ where $\hat{z}$ is the unit vector in the z direction. It is assumed that $\langle \underset{\sim}{B} \rangle$ satisfies a force-free model.

$$\nabla \times \langle \underset{\sim}{B} \rangle = \mu(r) \langle \underset{\sim}{B} \rangle \quad . \tag{7}$$

If μ were a constant, the solution would be

$$\langle B_z(x) \rangle = B_0 \cos \mu x \quad ,$$

$$\langle B_y(x) \rangle = B_0 \sin \mu x \quad . \tag{8}$$

In this model μ is allowed to be a function of x to obtain self-consistent currents and fields.

It is postulated that stochasticity is introduced by field fluctuations $\delta \underset{\sim}{B}(\underset{\sim}{r},t)$ that randomly move field lines across the plasma. Following Rosenbluth et al., /28/ a field line diffusivity, D_F, is introduced such that a particle following a field line a distance ℓ will undergo a mean square excursion in the x direction.

$$\langle (\Delta x)^2 \rangle \simeq 2 \ell D_F \quad . \tag{9}$$

The plasma is treated in the context of a Lorentz model where only electron-ion scattering is considered. For simplicity, it is assumed that electron guiding centers move along field lines, and the electron magnetic moment does not change between collisions. Unlike the Spitzer model /11/, the total momentum imparted to all electrons in a volume element by the electric field does not equal the momentum lost by electrons to collisions in the same volume element. For example, electrons near the $x = 0$ plane gain momentum faster than it is scattered away,

$$\eta_{\parallel} \langle J_z(0) \rangle < \langle E_z(0) \rangle \quad . \tag{10}$$

This happens because the mean-free path of an electron, λ, may be large enough to move the electron over significant portions of the plasma between collisions.

$$2\lambda D_F \sim a^2 \quad . \tag{11}$$

An electron may be accelerated in a region of high parallel field, $E_\parallel$, and move out of that region before it has a chance to scatter. Correspondingly, electrons may enter a region such as the reversal layer, $x = x_r$, where they lose more momentum to scattering than is gained from electric fields,

$$\eta_\parallel \langle J_y(x_r)\rangle > \langle E_y(x_r)\rangle = 0 \quad . \tag{12}$$

If the inequalities in Eqs. (10) and (12) are correct, there is a third possibility for an RFP profile sustainment mechanism.

A detailed description of the nonlocal resistivity is given in Ref. 27 and is beyond the scope of this paper. The key conclusions of Ref. 27 are given in Figs. (5) and (6). A Boltzman equation for electrons in a stochastic RFP was developed. A self-consistent example with field reversal was computed, using ZT-40M temperature, density, and confinement time data. The results shown in Fig. (5) indicate that field reversal can be maintained with a nonlocal resistivity. The level of stochasticity is described by $\lambda_0 D_F/a^2 = 0.05$ where λ_0 is the mean-free path for 90% scattering of electrons with the speed $v_0 = (2kT/m_e)^{1/2}$.

These data were obtained for ZT-40M parameters: electron temperature $T_e \simeq 200$ eV, density $n \simeq 10^{19} m^{-3}$, impurity level $Z_{eff} \simeq 1$, current $I_z \simeq 100$ kA, nonradiative energy containment time $\tau_{Ee} \simeq 200$ μs, mean-free path $\lambda_0 \simeq 40$ m, and field line diffusivity $D_F \simeq 5\times10^{-5}$ m. Since λ scales as $\lambda = \lambda_0(v/v_0)^4$, the high speed electrons are far more effective than thermal electrons in carrying current to the reversal layer. This allows λ_0 to be much smaller than indicated by Eq. (11).

Figure 6 illustrates how the reversal depends on $\lambda_0 D_F/a^2$. Although the information available to estimate $\lambda_0 D_F/a^2$ is subject to many approximations, /7/ the model is quite insensitive to the precise value of $\lambda_0 D_F/a^2$.

It should also be noted that field line stochasticity is sufficient to drive this RFP model but is not necessary. It is necessary that electrons wander stochastically through the plasma whether or not field lines do. There may even be instances in which perpendicular transport of electrons drives an RFP in the presence of good flux surfaces.

Interaction of Sustainment Models

In recent years, considerable effort has been spent to demonstrate: 1) that some type of "dynamo" effect is required in an RFP and 2) that a reasonable dynamo model exists. Now there is no doubt that a "dynamo" is necessary, and that there is an abundance of models to choose from. In this section we attempt to develop a relationship between the three models discussed previously.

If the MHD dynamo of Sec. 2.1 were acting alone to sustain an RFP in a steady "ohmic" state, one can establish minimum values for the field and current fluctuations using a quasi-linear model. The posibility of such an exercise was observed by Gerwin, Keinigs, and Schaffer. /30/

As an example, consider a slab model configured as in Sec. 2.3 with the mean fields in a Taylor state having reversal at the wall, $\mu a = \pi/2$. To be in an ohmic state, /17,18,19/ all physical variables are time independent functions of space. Therefore, the mean values, $\langle\ \rangle$, are taken to be spatial averages with x fixed, and the δ variations are three-dimensional functions that are time independent. It is assumed that there are no net radial flows and $\langle E_x \rangle$ is neglected, leading to $\langle \underline{u} \rangle = 0$. An isotropic Ohm's law is used, and no kinetic effects are invoked. Under these conditions, Eq. (3) is rewirtten,

$$\langle \underline{E} \rangle + \delta \underline{E} = \eta(\langle \underline{J} \rangle + \delta \underline{J}) - \delta \underline{u} \times \langle \underline{B} \rangle - \langle \delta \underline{u} \times \delta \underline{B} \rangle \quad . \tag{13}$$

Equation (13) can be separated into mean and fluctuating parts

$$\eta \langle \underline{J} \rangle - \langle \underline{E} \rangle = \langle \delta \underline{u} \times \delta \underline{B} \rangle \tag{14}$$

and

$$\delta \underline{E} = \eta \delta \underline{J} - \delta \underline{u} \times \langle \underline{B} \rangle \quad . \tag{15}$$

The fundamental premise of the model is that the quadratic term $\langle \delta \underline{u} \times \delta \underline{B} \rangle$ will make up the difference between $\eta \langle \underline{J} \rangle$ and $\langle \underline{E} \rangle$ everywhere in the plasma. The time independent nature of the model requires $\partial \underline{B}/\partial t = -\nabla \times \underline{E} = 0$,

therefore, the curl of Eq. (15) must be zero. This curl condition establishes a relationship between $\delta\underline{u}$ and $\delta\underline{B}$.

We assume that $\delta\underline{u}$ can be expanded in a Fourier series

$$\delta\underline{u}(\underline{r}) = \sum_{\underline{k}} \delta\underline{u}(\underline{k}) e^{i\underline{k}\cdot\underline{r}} \quad . \tag{16}$$

Likewise $\langle\underline{B}\rangle$ can be written as follows

$$\langle\underline{B}\rangle = \underline{B}_{+} e^{i\underline{\mu}\cdot\underline{r}} + \underline{B}_{-} e^{-i\underline{\mu}\cdot\underline{r}} \quad , \tag{17}$$

where $\underline{\mu} = \mu\hat{x}$ and $B_{\pm} = 1/2\ B_0(\hat{z} \mp i\hat{y})$. It can be shown from the curl of Eq. (15) that for every Fourier component $\delta\underline{u}(\underline{k})$ there are two Fourier components of $\delta\underline{B}$,

$$\delta\underline{B}_{\pm}(\underline{k}) = (\mu_0 i/\eta k_{\pm}^2) \{(\underline{k}_{\pm}\cdot\underline{B}_{\pm})\delta\underline{u}(\underline{k}) - [(\underline{k}_{\pm}\cdot\delta\underline{u}(\underline{k})]\underline{B}_{\pm}\} \quad , \tag{18}$$

where $\underline{k}_{\pm} = \underline{k} \pm \underline{\mu}$.

We consider the simple example $\delta\underline{u}(\underline{k}) = u_0(\hat{x}+i\hat{z})$ with $\underline{k} = k\hat{y}$, to solve the y component of Eq. (14),

$$\eta\langle J\rangle_y = (\eta\mu B_0/\mu_0) \sin \mu x$$

$$= \langle\delta\underline{u} \times \delta\underline{B}\rangle_y = \frac{1}{2} \mathrm{Re} \langle\delta\underline{u}(\underline{k},x) \times [\delta\underline{B}_{+}^{*}(\underline{k}_{+},x) + \delta\underline{B}_{-}^{*}(\underline{k}_{-},x)]\rangle_y \quad . \tag{19}$$

The corresponding volume averaged minimum of field fluctuations squared is

$$\frac{\mu k}{2(k^2+\mu^2)} \leq \int_{-a}^{a} \langle\delta B^2\rangle dx / \int_{-a}^{a} \langle B\rangle^2 dx \quad . \tag{20}$$

When a similar estimate of power dissipation in fluctuations is made we get

$$\frac{k}{2\mu} < \int_{-a}^{a} \eta\langle \delta J^2\rangle dx \Big/ \int_{-a}^{a} \eta\langle J\rangle^2 dx \quad . \tag{21}$$

There are many caveats that enter into Eqs. (20) and (21); the most important are the slab model in a Taylor state, isotropic resistivity, and incompressible flow. The momentum equation was not required for the exercise. We assumed a velocity flow that would produce the most efficient dynamo in the y direction. To the best of our knowledge, adding momentum and the z direction dynamo will increase the inequalities of Eqs. (20) and (21). The left-hand sides of Eqs. (20) and (21) may be reduced by having: $\eta_\perp/\eta_\parallel >> 1$, compressible flow, less dynamo action as in the MBFM, and/or a variable resistivity $\eta(x)$. We do not expect dramatic changes in Eqs. (20) and (21), provided $\eta_\perp$ does not greatly exceed $\eta_\parallel$ as in the TDM.

If the models leading to Eqs. (20) and (21) are reasonably correct, there are significant implications for ohmic states and sustainment modeling as a whole. It was noted in Ref. 10 that $|\delta\underset{\sim}{B}|/\langle B\rangle$ at the plasma edge is $\lesssim$ 5% in ZT-40M, and it was assumed that the volume averaged fluctuations are comparable. It was also estimated in Ref. 10 that fluctuation power divided by mean field dissipation is about 40% in ZT-40M. Equations (20) and (21) combined with these data would indicate

$$\frac{k}{\mu} \lesssim 5 \times 10^{-3} \quad . \tag{22}$$

For $a = 0.2$ m as in ZT-40M, this would say that an ohmic state must have a wavelength greater than ~ 160 m, or $|\delta\underset{\sim}{B}|/\langle B\rangle$ must be significantly greater than estimated in Ref. 10. A 160 m ohmic state wavelength is much greater than the machine dimensions and quite unrealistic. However, computer models have generated specific ohmic states with wavelengths on the order of ~1 m and $|\delta\underset{\sim}{B}|/\langle B\rangle$ ~ 10% /18,19/. There is also experimental evidence of some internal structure that may relate to ohmic states /31/.

The concern over the inconsistency between an ohmic state model and experimental results worsens when fluctuations are observed to decrease at higher currents, $|\delta\underset{\sim}{B}|/\langle B\rangle|_{r=a}$ ~1% /32/. If it becomes more difficult to reconsile experimental results with ohmic states, one must invoke a more

general theoretical model. For instance the steady state assumption of the ohmic model can be dropped. If a time dependent MHD model has good flux surfaces, this author believes Eqs. (20) and (21) will still hold, but that point of view remains to be proven.

If, on the other hand, the magnetic field becomes stochastic and time dependent, we cannot be sure of Eqs. (20) and (21). Indeed, if stochastic fields become a part of the dynamo model one should go on to consider nonlocal resistivities as discussed in Sec. 2.3.

4. Conclusions

We have briefly described RFP profile sustainment by means of the MHD dynamo, the tangled discharge model, and nonlocal resitivity. Treating time independent ohmic states as a subset of the MHD dynamo, we have placed lower bounds on the field fluctuations (departures from symmetry) consistent with states of a given wavelength, k. On comparing our theory to experimental results, we find it difficult but not impossible to reconcile ohmic states with experiment. We recommend that more detailed field fluctuation data inside the plasma be sought. The associated large wavelength field fluctuations should be observable. If the conditions of ohmic states cannot be met, the field will probably be stochastic. In that event, MHD activity would establish stochasticity that would play a significant role in profile sustainment through nonlocal resistivity. In turn, field line stochasticity would substantially affect particle and thermal transport within the plasma. Since dynamo action is reduced near the wall in some models, MBFM, stochasticity may also be low near the wall. Consequently, particle and thermal losses from the machine may be a boundary layer phenomenon closely coupled to the process of RFP profile sustainment.

Acknowledgment

The author wishes to express his appreciation to D. A. Baker, J. M. DiMarco, R. A. Gerwin, A. R. Jacobson, G. Miller, R. A. Nebel, M. Schaffer, K. F. Schoenberg and L. Turner for many helpful discussions.

References

/1/ BODIN, H.A. and NEWTON, A.A., Nucl. Fusion, 20 (1980) 1255.

/2/ BAKER, D.A. and QUINN, W.B., "The Reversed-Field Pinch," Fusion, 1, Part A, Chapter 7, E. Teller, Editor, Academic Press, Inc., New York, NY (1981).

/3/ ROBINSON, D.C., Plasma Phys., 13 (1971) 439.

/4/ COLGATE, A.A., FERGUSON, S.P., and FURTH, H.P., Proc. U. N. Conf. on Peaceful Uses of Atomic Energy, 32 (1958) 129.

/5/ TAYLOR, J.B., Phys. Rev. Lett., 33 (1974) 1139.

/6/ BAKER, D.A., et al., "Performance of the ZT-40M Reversed-Field Pinch With an Inconel Liner," Plasma Phys. and Controlled Nucl. Fusion Research 1982 Intl. At. Energy Agency, Vienna, Vol. II (1983) 587.

/7/ JOHNSTON, J.W., Plasma Phys., 23 (1981) 187.

/8/ SCHOENBERG, K.F., GRIBBLE, R.F., and PHILLIPS, J.A., Nucl. Fusion, 22 (1982).

/9/ TAMANO, T., et al., "Pinch Experiments in OHTE," Plasma Phys and Controlled Nucl. Fusion Research 1982, Intl. At. Energy Agency, Vienna, Vol. I, (1983).

/10/ SCHOENBERG, K.F., MOSES, R.W., and HAGENSON, R.L., "Plasma Resistivity in the Presence of a Reversed-Field Pinch Dynamo," to be published in Phys. Fluids, 27 (July 1984).

/11/ SPITZER, L., Physics of Fully Ionized Gases, Wiley, New York, NY (1962).

/12/ TURNER, L. and CHRISTIANSEN, J.P., Phys. Fluids, 24 (1981) 893.

/13/ TURNER, L., Ann. Phys., 149 (1983) 58.

/14/ CARAMANA, E.J. and BAKER, D.A., Nucl. Fusion, 24 (1984) 423.

/15/ CARAMANA, E.J. and MOSES, R.W., Nucl. Fusion, 24 (1984) 498.

/16/ MOFFATT, H.K., Magnetic Field Generation in Electrically Conducting Fluids, Cambridge University Press, Cambridge, England (1978).

/17/ SYKES, A. and WESSON, J.A., Phys. Rev. Lett., 37 (1978) 140.

/18/ SCHNACK, D.D., Proc. RFP Theory Workshop, Los Alamos National Laboratory report LA-8944-C (1980) 118.

/19/ AYDEMIR, A.Y. and BARNES, D.C., Phys. Rev. Lett., 52 (1984) 930.

/20/ CARAMANA, E.J., NEBEL, R.A., and SCHNACK, D.D., Phys. Fluids, 26 (1983) 1306.

/21/ WATT, R.G. and NEBEL, R.A., Phys. Fluids, 26 (1983) 1168.

/22/ WERLEY, K., NEBEL, R.A., and WURDEN, G.A., "Transport Description of the Risetime of Sawtooth Oscillations in RFPs," submitted to Phys. Fluids (1984).

/23/ STRAUSS, H.R., "Dynamical Equations for the Reversed-Field Pinch," to be published in Phys. Fluids, 27 (1984).

/24/ SCHNACK, D.D., et al., "Three-Dimensional Magnetohydrodynamic Studies of the Reversed-Field Pinch," submitted to Phys. Fluids, (May 1984).

/25/ MILLER, G., Los Alamos National Laboratory report LA-UR-83-2888 (1983).

/26/ RUSPRIDGE, M.G., Plasma Phys., 19 (1977) 499.

/27/ JACOBSON, A.R. and MOSES, R.W., "Nonlocal dc Electrical Conductivity of a Lorentz Plasma in a Stochastic Magnetic Field," to be published in Phys. Rev. (July 1984).

/28/ ROSENBLUTH, M.N., et al., Nucl. Fusion, 6 (1966) 297.

/29/ RECHESTER, A.B. and ROSENBLUTH, M.N., Phys. Rev. Lett., 40 (1978) 38.

/30/ GERWIN, R.G., KEINIGS, R., and SCHAFFER, M., private communication (1983).

/31/ WURDEN, G.A., Phys. Fluids, 27 (1984) 551.

/32/ BAKER, D.A., private communication (1984).

Figure Captions

Fig. 1 An isometric view of the RFP field and current profiles during the sustained phase of the discharge. $\underset{\sim}{P}_s$ represents the steady state Poynting vector carrying power to the central region of the plasma. Mean field power absorption $\langle\underset{\sim}{J}\rangle\cdot\langle\underset{\sim}{E}\rangle$ is maximized in the central discharge region because $\langle\underset{\sim}{J}\rangle$ is parallel to the applied toroidal electric field $\langle\underset{\sim}{E}\rangle$. Hypothetically, the mean power absorbtion is partially converted to fluctuating fields ($\underset{\sim}{P}_d$) that drive the poloidal plasma currents via the dynamo effect.

Fig. 2 An experimental F - Θ curve for a 180 kA discharge in ZT-40M compared to the BFM prediction (solid curve).

Fig. 3 The Modified Bessel Function Model (MBFM) magnetic field profiles for a given $\mu(r)$.

Fig. 4 An experimental F - Θ curve for a 180 kA discharge in ZT-40M compared to the MBFM prediction (solid curve).

Fig. 5 Magnetic-field components and parallel current density versus x, with $\lambda_0 D_F/a^2 = 0.05$. Each curve is normalized to 1 at x = 0.

Fig. 6 $B_z(a)/\langle B_z\rangle$ versus $B_y(a)/\langle B_z\rangle$ for various $\lambda_0 D_F/a^2$.

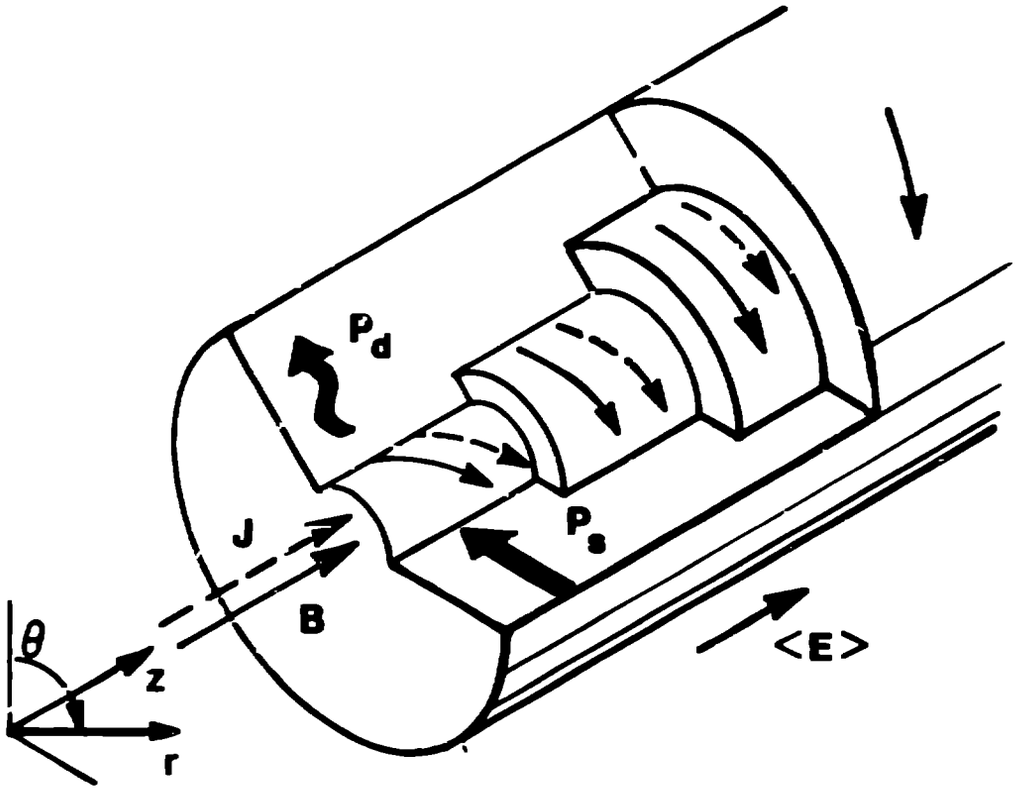

Figure 1

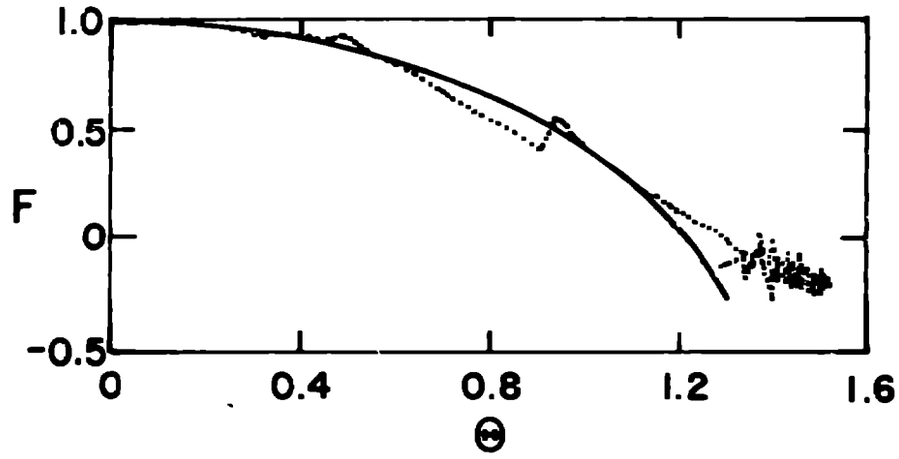

Figure 2

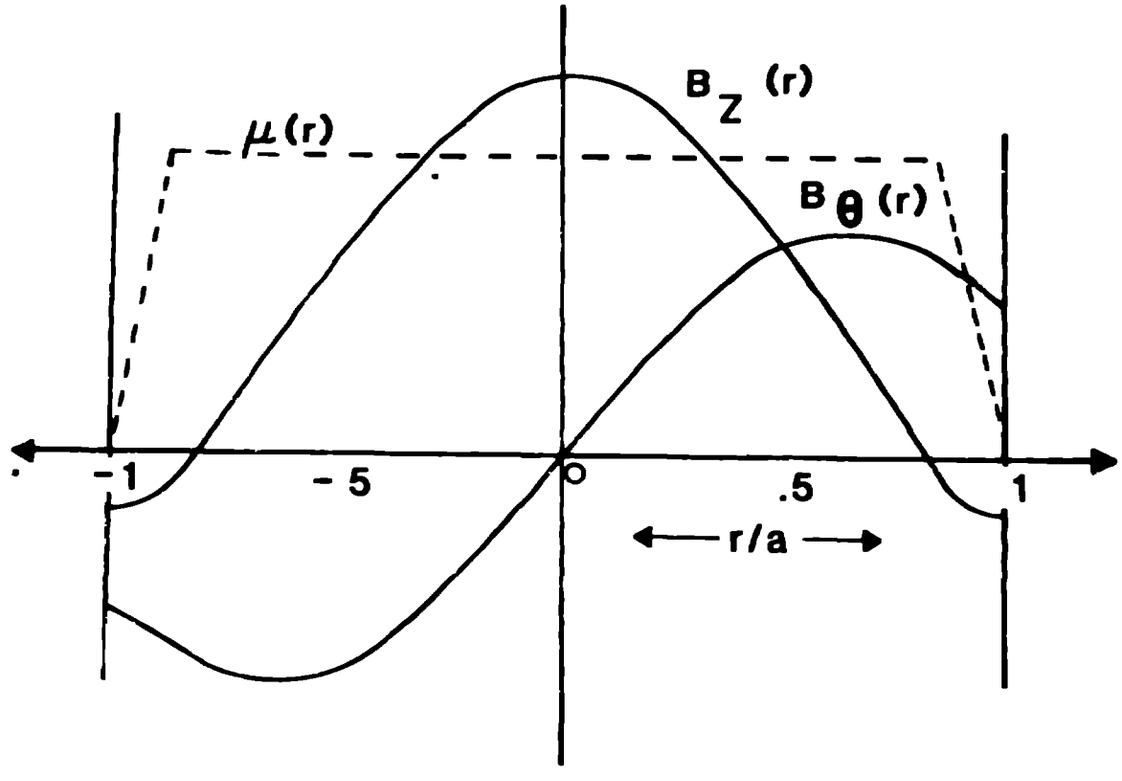

Figure 3

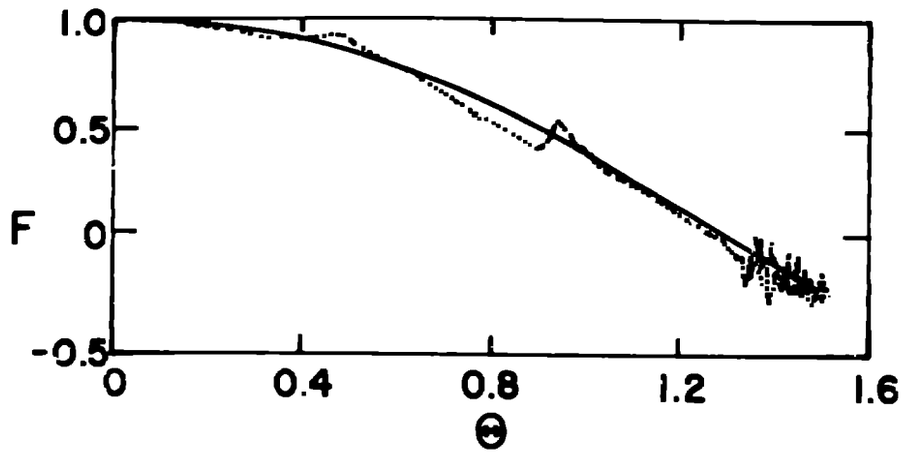

Figure 4

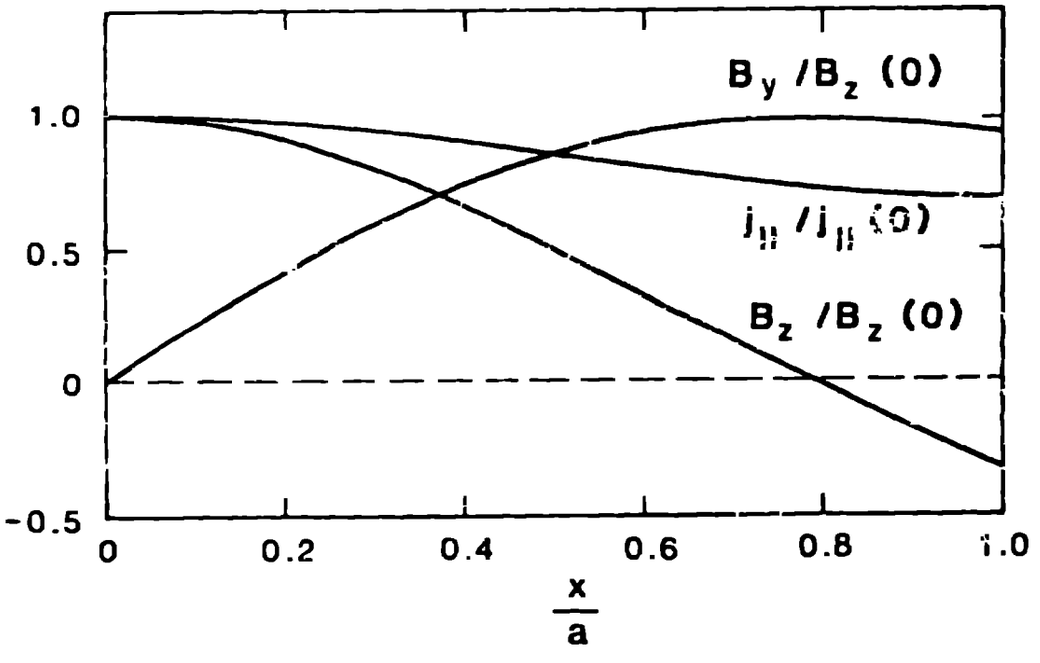

Figure 5

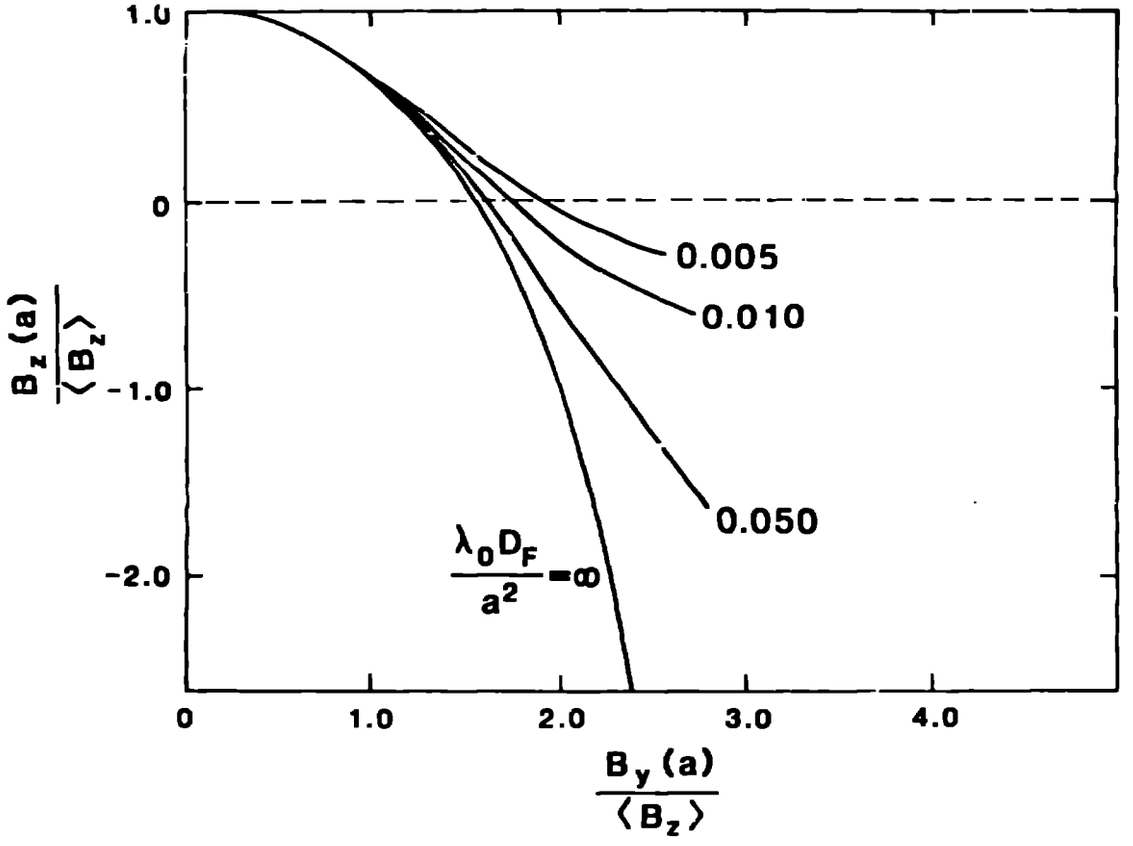
1.0
0
-1.0
-2.0
0
1.0
2.0
3.0
4.0
$\frac{B_z(a)}{\langle B_z \rangle}$
$\frac{B_y(a)}{\langle B_z \rangle}$
0.005
0.010
0.050
$\frac{\lambda_0 D_F}{a^2} = \infty$

Figure 6